Journal of the Arkansas Academy of Science

Volume 44 Article 7

1990

Rotational Symmetries of Nuclear States: Spin Determinations in Advanced Laboratory

Wilfred J. Braithwaite
University of Arkansas at Little Rock

ROTATIONAL SYMMETRIES OF NUCLEAR STATES: SPIN DETERMINATIONS IN ADVANCED LABORATORY

W.J. BRAITHWAITE
Department of Physics and Astronomy
University of Arkansas at Little Rock
Little Rock, AR 72204

ABSTRACT

An advanced laboratory experiment is described which shows the connection between the rotational symmetries of nuclear states and the assignments of spins to discrete nuclear states. Standard angular correlation methods were used to study the two sequential gamma ray transitions in each ^{60}Ni nucleus, populated by unobserved beta decays from a weak radioactive ^{60}Co source. The chosen electronics and detectors were inexpensive and easy to operate. This experiment was extended to introduce students to real-world data acquisition, using finite-geometry detectors, which resulted in enormously larger coincident data rates.

INTRODUCTION

Many advanced students in the physical sciences are introduced to the idea of the spin quantum number (J) of a state determining the symmetry of the state under spatial rotation (Brink and Satchler, 1968; Ferguson, 1965; Cramer and Eidson, 1964; Edmonds, 1960). However, this idea is rarely given a tangible counterpart in the laboratory. To correct this, a correlation experiment was sought, emphasizing clarity in experimental design while minimizing the need for expensive equipment.

The choice was narrowed to gamma-ray de-excitation of nuclear states, due to the large specific energies, resulting in very penetrating photons, thus, avoiding absorption corrections. Also, fairly small (7.62 cm x 7.62 cm) Sodium Iodide (NaI) detectors are fairly inexpensive, and their responses to gamma rays of wide energy range are well documented in the literature.

The experiment chosen was the measurement of angular correlations between two gamma rays, corresponding to sequential transitions in each ^{60}Ni nucleus, populated by unobserved beta decays from a weak radioactive ^{60}Co source. Figure 1 shows the decay scheme. Both

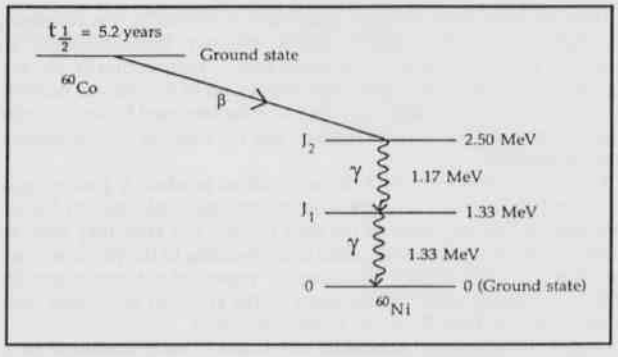

Figure 1. Decay scheme for radioactive ^{60}Co.

gamma rays are very penetrating, but have an average full-energy detection efficiency (peak-to-total ratio) of 36% in these small (7.62 cm x 7.62 cm) NaI detectors.

In this experiment, the second-excited state (spin = J_2) of ^{60}Ni decays by single gamma-ray emission to its first-excited state (spin = J_1) which decays by single gamma-ray emission to its ground state (spin = 0). The principal experimental goal was to distinguish between the different angular-correlation predictions for the two gamma rays, associated with different possible assignments of J_2 and J_1.

Eight distinct angular functions were calculated (Evans, 1955) for 11 different reasonable values for the nuclear spins: J_2 and J_1. Agreement between the angular correlation data and one of the predictions could provide unique assignments for J_2 and J_1, based on the expectation of a unique rotational symmetry associated with each of these discrete states (Brink and Satchler, 1968; Eisenbud and Wigner, 1958).

Perhaps as important for the student was the sense of "no guarantee" that the data would agree with any of these predictions, if there were some fundamental problem with quantum mechanics. The students showed anticipation in experimentally testing quantum mechanics by using its predictions in their attempt to extract spin quantum numbers.

Finally, students compared the situation of "point-geometry" predictions at distant detector settings with low counting rates to the situation of "finite geometry" predictions for close-in detector settings with much higher counting rates.

This comparison confronted students with experimental realities. They could take data with detectors at 20 cm, and come in every 12 hours to change angle (as they wanted statistical accuracy of 1%), or they could take data with detectors at 5 cm (at measured coincidence rates over 50 times as fast), and finish each run in 15 minutes. They could use the simple "point geometry" predictions at 20 cm, but they would have to make corrections in the predictions to compensate for "finite geometry" in the detectors at 5 cm.

Since the students had estimated in a rough calculation that the "finite geometry" correction was negligible at 20 cm, they decided, as an initial strategy, to set the detectors 20 cm from the source and read out the data about every 12 hours for 7 data points between 90 and 180 degrees, but taking 4 times longer at 90 degrees, so W(90°) would be well determined when forming the ratios: $W(\Theta)/W(90°)$.

Having established the spins, J_2 and J_1, using the point-geometry predictions, students decided to re-run the whole experiment at the 5 cm settings. New runs came in as fast as the students could plot their results. The anisotropy in each of the angular correlations was reduced, but students calculated new values for each candidate, and the spins were established in less than one-fiftieth of the 20-cm data-collection time.

The reason for re-doing the experiment was posed in more than 1 way. (1) With the spins established, re-doing the experiment allowed the student to check the accuracy of his finite-geometry corrections. (2) If this were an experiment being designed for a large accelerator facility, finite geometry work would be vital so as not to waste precious time on a very expensive machine. No Program Advisory Committee would tolerate point geometry with finite geometry measurements 50 times faster.

Students had no trouble viewing their work both ways. They realized the present apparatus as not expensive to run, and was not in high demand, so they were more comfortable in making their first com-

parisons without modifying the predictions for finite geometry. However, they understood the need to be able to make "real world" measurements, and they were quite amazed at the difference in data collection times.

MATERIALS AND METHODS

Figure 2 shows the point-geometry predictions for 11 different combinations of excited-state spins and de-excitation gamma ray multipolarities, the latter given in parentheses. It also shows results for data taken with the two 7.62 cm x 7.62 cm NaI detectors placed 20 cm from the source.

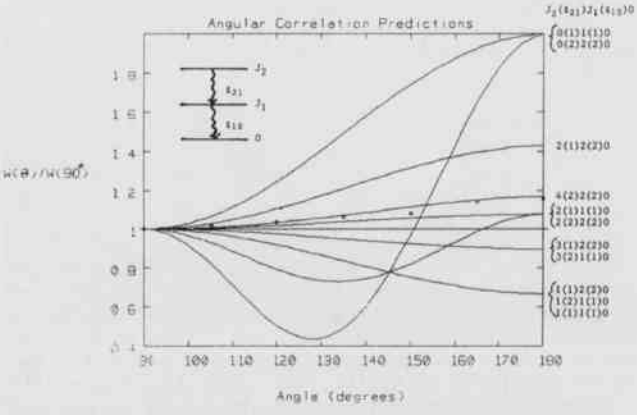

Figure 2. Predictions for eleven different combinations of excited state spins and de-excitation gamma ray multipolarities, the latter given in parenthesis. Data for ^{60}Ni are the small boxes.

The ^{60}Co source was a combination of 6 plastic disk sources, wrapped together to form a short cylinder, and placed equidistant from the two detectors: one being fixed at 0° and the other mounted on a movable arm. One percent statistical accuracy was intended, so 2 procedures were used to make systematic errors negligible.

A stick was cut as a template to assure the movable detector would be the same distance from the source, independent of angle. This procedure was carried out before any data acquisition, with the detector distances checked for angles between 90° and 180°. In addition, the cylindrical source was rotated, and the singles rates for the 1.33 MeV full-energy peak were measured to assure there was no favored orientation due to poor source positioning within the disks.

The half-life of the ^{60}Co is 5.2 years, so measurements taken over a 1 week interval could be normalized to clock time. The present sources add up to about 1 micro-Curie of activity, easily determined by singles measurements in either detector.

One of the 2 NaI detectors was equipped with a mu-metal shield on its photo-multiplier tube. This detector was used on the movable arm, so it would be insensitive to changes in the earth's magnetic field when placed in different orientations. Students appreciated the mu-metal shield when they observed the dramatic change in gain on the oscilloscope display of the singles pulses, when a small bar magnet (with a magnetic field much larger than the earth's field) was moved near the unshielded phototube, in contrast to the nearly negligible change in gain when the magnet was moved near the shielded phototube.

Figure 3 is a diagram of the electronics used to process linear energy signals from each NaI detector. The anode output of each phototube was sent through a voltage-sensitive, unit-gain preamplifier without changing its time response (about 10 nanoseconds rise time and 50 microseconds decay time).

The output of each preamplifier was sent to an RC shaping amplifier which produced a bipolar pulse whose crossover time is insensitive to the pulse height. Each bipolar linear energy signal was split into 2 paths: One was sent to a timing single channel analyzer (SCA) which required

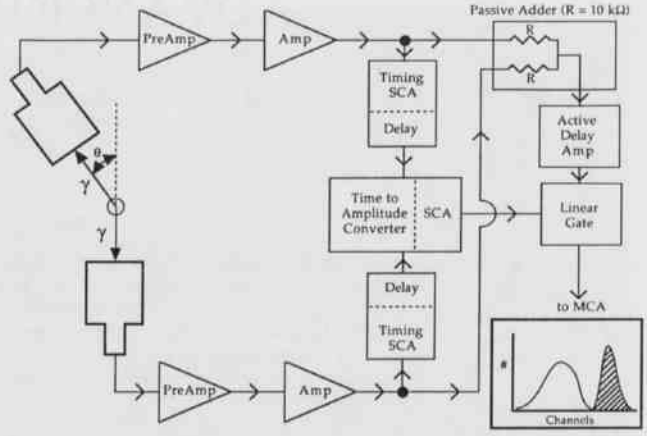

Figure 3. Electronics diagram for gamma-gamma coincidence using small Sodium Iodide detectors. SCA (single channel analyzer), MCA (multi channel analyzer).

the linear pulse to cross a lower threshold (but be less than an upper threshold) before a logic pulse was generated at the crossover time. The other signal was sent to a passive (resistive) mixer.

Each SCA output logic pulse was sent to an electronic unit to determine whether there were simultaneous signals present from both NaI detectors. This could have been accomplished using an overlap slow coincidence unit, but we chose to use a time-to-amplitude converter (TAC) with an internal timing single channel analyzer. The TAC provides the student a much clearer view of the coincidence process, as may be seen below.

The TAC produced a linear signal proportional to the difference in time between the 2 logic signals from the 2 SCAs, where the latter were separated by an artificial delay of about 100 nanoseconds, set using the internal delays of the SCAs.

The TAC linear output could be inhibited using its internal SCA, so both upper and lower gates could be set around the "true" coincidence time peak, which sat above a very small (but observable) accidental background. The upper and lower SCA gates of the TAC were set with 10-turn helipots, and their positions were calibrated by measuring their effect on the TAC linear signal, initially sent (for calibration purposes) to a multichannel analyzer (MCA).

The amplitude of each linear signal sent to the MCA was converted to a digital value by its analog-to-digital converter. The horizontal scale displayed channel numbers, corresponding to monotonically increasing values of the digitized signal. The population of the channel number, corresponding to each digitized pulse, was incremented by one for each pulse processed. The vertical display was the readout of this population per channel.

The SCA helipots of the TAC were set to produce a gating signal for a time difference corresponding to the time peak (due to "true" coincidences) during most of the data taking. But later they were set to produce a gating signal for pulses corresponding to the very low counting rate (flat distribution) "accidental" region of the time spectrum, allowing a quantitative measurement of the effect of accidental coincidences on the final $E_1 + E_2$ coincidence data.

Using this technique, accidental coincidences were measured to be less than 2%. This meant they could be ignored, since accidental rates only affect the anisotropy [W(Θ)/W(90°) - 1]. A 1% measurement of the yield ratio means determining a 16% anisotropy to 6% (and a 10% anisotropy to 10%), so the effect of accidentals on the anisotropy is less than the statistical error.

The internal SCA of the TAC was used to generate the gating signal for the linear gate, which passed pulses from the mixer only when a true coincidence was present. This device took about 2 microseconds to make this electronic decision, so the output of the passive mixer was routed through an active delay amplifier, which produced a delayed linear output.

The delayed signal from the mixer was sent to the linear gate. When an SCA logic pulse from the TAC was present, the linear gate opened, permitting the linear pulse to pass. This only occurred when there were simultaneous signals present from both detectors. The mixer signal was passed through the linear gate only when signals from both detectors were present. Thus, the mixer operated as a linear adder of each detector's linear energy signal, so the output of the linear gate was proportional to $E_1 + E_2$, when the gains of the two detectors were matched.

Figure 4 is an example of a gamma-ray "singles" spectrum, taken with either NaI detector. The vertical population index was incremented for the horizontal scale corresponding to energy deposition in the detector, for each singles event. The 2 sharp peaks correspond to full-energy deposition of 1.17 MeV and 1.33 MeV gamma rays, arriving asynchronously, in each detector.

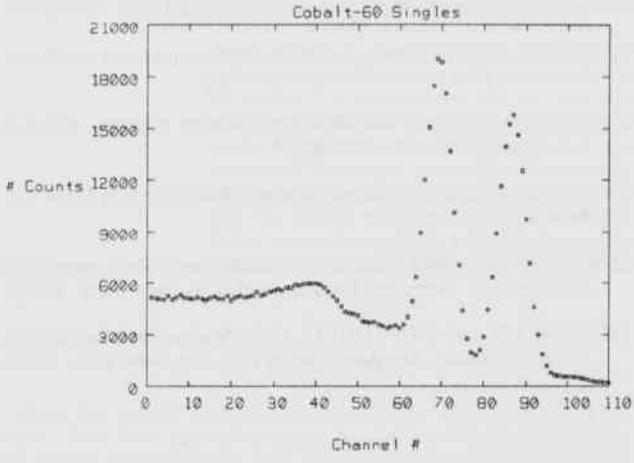

Figure 4. Gamma ray singles from either small NaI detector.

Each full-energy peak was separated from the most energetic Compton scattering for that gamma ray. Thus, when there was a true coincidence between the 2 detectors, and each detector measured the full-energy of the gamma ray, the sum peak had the fixed value of: $E_{sum} = E_1 + E_2 = 1.17$ MeV + 1.33 MeV = 2.50 MeV. If 1 of the detectors had full-energy deposition while the other had a Compton scattering, the event was processed in the spectral region below the sum energy peak. Figure 5 is a sum energy spectrum, formed with the linear gate opened only for true coincidences. The sum energy peak is well resolved on the right, where the broad spectrum on the left was incremented if one or both of the gamma rays escaped (not yielding full energy).

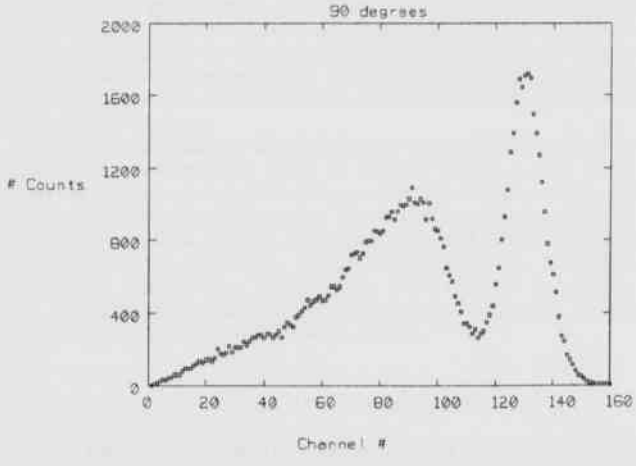

Figure 5. Coincidence gamma-gamma sum spectrum for ^{60}Ni.

Gain matching between the 2 detectors was carried out using the MCA and a slight (temporary) modification in the electronics. For each detector, the positive logic output of each SCA was used to open the linear gate, so the mixed signal passed would come from only 1 of the detectors, depending on which SCA was being used to open the linear gate.

Once the gain of one of the detectors was adjusted to give a suitable display in the MCA, the other SCA was used to open the linear gate, passing the singles pulses from the other detector. The amplifier gain was adjusted until the centroids of the 1.17 MeV and the 1.33 MeV peaks agreed within 0.3 channels of those in the first detector. A gaussian fitting routine in the computer based MCA was used to determine these centroids, but the use of overlap spectra (usually available in MCAs) works about as well in matching the relative gains.

Since the statistical error was chosen to be less than 1% in determining the ratio of $W(\Theta)/W(90°)$, systematic errors must be kept below 1% also. Thus, the method for determining the number of counts in the sum energy peak was examined, since extracting peak areas to better than 1% accuracy is not a trivial feat. Fortunately, only the ratios $N(\Theta)/N(90°)$ were needed to better than 1%. This should be assured if each area (both numerator and denominator) were determined in a consistent way, as each Compton background was nearly proportional to the sum peak area. In order to be able to test for consistency in determining each ratio, 2 different methods were used: summing the populations within the sum peak and fitting the sum peak to a gaussian.

Both methods impressed the students with the need for gridding the sum peak over many channels (20 or more) for both methods of peak extraction: (1) so the error in the summing technique would not sensitively depend on the cutoff channels, and (2) so the gaussian fitting procedure would have enough data points to allow the extraction of a reliable area.

Had they demanded less statistical accuracy, the students would have missed the opportunity to overcome the systematic difficulties in extracting peak areas. Also, their determination of spins would have been less certain. Having faced and overcome these problems, the students seemed proud of their newly acquired experimental skills.

RESULTS

The data points in Figure 2 are to be compared with the point geometry predictions of the various candidate angular correlation functions. A similar graph for finite geometry could have been included, but it differs very little from Figure. 2, except the anisotropies are smaller (like a squeezed accordion).

Correcting the predicted angular correlation functions for the finite geometry of the gamma-ray detectors was accomplished easily when the correlation functions are written as $W(\Theta) = a_0 + A_2P_2(\cos\Theta) + a_4P_4(\cos\Theta) + a_4P_4(\cos\Theta)$, where the P_{2L} functions are the ordinary Legendre polynomials. Published correction factors for the a_{2L} coefficients are available (Marion and Young, 1968). For the 5 cm positions, each a_2 is reduced by the factor 0.6496 and each a_4 is reduced by the factor 0.2116.

The source of the 11 different angular correlation functions (Evans, 1955) listed them as $W(\Theta) = b_0 + b_2\cos^2\Theta + b_4\cos^4\Theta$. Because of this, it is convenient to be able to relate each set of a_{2L} coefficients to the b_{2L} coefficients: $a_4 = (8/35)\, b_4$, $a_2 = (4/7)\, b_4 + (2/3)\, b_2$, and $a_0 = (1/5)\, b_4 + (1/3)\, b_2 + b_0$, using the orthogonality properties of Legendre polynomials (Boas, 1983).

As an example, using the 4(2)2(2)0 transitions, finite geometry corrections for the ratio $R = W(180°)/W(90°)$ give the following values: (1) For detectors 20 cm from the ^{60}Co source, R = 1.159, instead of 1.167 for point geometry, and (2) For detectors 5 cm from the ^{60}Co source, R = 1.103.

DISCUSSION

Students showed interest in the idea of connecting rotational symmetry properties of nuclear states to measured angular correlation functions, as determined by the spin quantum numbers of these states. They seemed most comfortable with references (e.g., Cramer and Eidson,1964) using the rotation matrix to calculate the angular correlations directly, as they could see the connection between the spin quantum number in the rotation matrix and the angular dependence of the rotation matrix. This may have been due in part to their seeing plots of the rotation matrices (Cramer and Braithwaite, 1972), as well as the connection between simple rotation matrices and Legendre polynomials (Braithwaite, 1973; Braithwaite and Cramer, 1972).

Students seemed to find this a particularly enjoyable lab, despite the considerable effort it required of them.

ACKNOWLEDGMENT

Thanks are extended to Dr. Richard Prior for his suggestion of using ^{60}Co in conjunction with the published list of 11 candidate angular correlation functions (Evans, 1955). Also, thanks are extended to Dr. Andre' Rollefson for his suggestion of incorporating the finite geometry measurements into this laboratory experiment, and for his many helpful comments during the writing of this manuscript.

LITERATURE CITED

BOAS, M.L. 1983. Mathematical methods in the physical sciences. John Wiley & Sons, New York. 793 pp.

BRAITHWAITE, W.J. and J.G. CRAMER. 1972. The reduced rotation matrix. J. Computer Phys. Comm. 3:318-321.

BRAITHWAITE, W.J. 1973. Associated legendre polynomials, ordinary and modified spherical harmonics. J. Computer Phys. Comm. 5:390-394.

BRINK, D.M. and G.R. SATCHLER. 1968. Angular momentum. Clarendon Press, Oxford, 160 pp.

CRAMER, J.G. and W.W. EIDSON. 1964. Angular correlations and nuclear polarization from the inelastic scattering of alpha particles. Nuclear Phys. 55:593-612.

CRAMER, J.G. and W.J. BRAITHWAITE. 1972. The reduced rotation matrix: plots and zeros. Nuclear Data Tables A10:469-476.

EDMONDS, A.R. 1960. Angular momentum in quantum mechanics. Princeton Univ. Press, Princeton, 146 pp.

EISENBUD, L. and E.P. WIGNER. 1958. Nuclear structure. Princeton Univ. Press, Princeton, 128 pp.

EVANS, R.D. 1955. The atomic nucleus. McGraw-Hill Book Co., New York, 972 pp.

FERGUSON, A.J. 1965. Angular correlation methods in gamma-ray spectroscopy. American Elsevier Publ. Co., New York, 214 pp.

MARION, J.B. and F.C. YOUNG. 1968. Nuclear reaction analysis, graphs and tables. American Elsevier Publ. Co., New York, 169 pp.